한국지반공학회논문집 제19권 6호 2003년 12월 pp. 161 ~ 168

Analysis of Steep Cuts and Slopes in Cemented Sand Using Fracture Mechanics

파괴역학을 이용한 경화모래로 이루어진 사면의 해석

Kim, Tae-Hoon[*1] 김 태 훈
Kang, Kwon-Soo[*2] 강 권 수
Lee, Jong-Cheon[*3] 이 종 천

요 지

대부분의 자연상태의 사질토는 어느 정도 경화되어 있다. 경화의 정도는 흙의 체적변형 거동이나 강도에 중요한 영향을 준다. 경화된 사질토 지반의 중요한 특징은 사질토임에도 불구하고 굉장히 높이 서 있을 수 있다는 것이다. 많은 현장 관측이나 경화모래로 된 사면의 파괴 해석들은 기존의 사면해석방법이 적절하지 않다는 것을 보여준다. 이것은 단지 파괴면이 원호가 아니라는 점 뿐만 아니라 파괴면에서의 전단응력이 실험으로부터 얻어진 전단강도보다 훨씬 작기 때문일 것이다. 이러한 사실은 파괴양상이 Mohr-Coulomb 전단파괴와 다르다는 것을 말한다. 이런 파괴는 파괴역학 개념과 이론으로 설명될지도 모른다. 이 논문에서는 파괴역학 개념을 이용해서 경화모래로 이루어진 급경사 사면의 해석을 수행하였다. FEM 해석 결과는 파괴역학의 개념을 이용한 해석방법이 경화사질토로 이루어진 지반구조물의 설계나 안정해석에 훌륭한 대안임을 보여주고 있다.

Abstract

Most natural deposits of sandy soil possess some degree of cementation resulting from the deposition and precipitation of cementing agents. The presence of cementation can have a significant influence on the stiffness and volume change behavior, and the strength of soils. An important feature of deposits of cemented sandy soils is their ability to remain stable in surprisingly high and almost vertical man-made cuts as well as natural slopes. Numerous field observations and studies of failures in slopes of cemented soils have reported that application of conventional analysis techniques of slope stability is inadequate. That is not only due to the fact that the failure surface of the slope is not circular, but also the fact that the average shear stress along the failure surface is much smaller than the shear strength measured in laboratory shear experiments. This observation alerts us to the fact that a mechanism different from conventional Mohr-Coulomb shear failure takes place, which may be related to fracture processes, which in turn are governed by fracture mechanics concepts and theory. In this study, steep slopes in cemented sand were assessed using fracture mechanics concepts. The results showed that FEM coupled with fracture mechanics concepts provides an excellent alternative in the design and safety assessment of earth structures in cemented soils.

Keywords : Cementation, FEM, Fracture mechanics, Mohr-Coulomb, Slopes

*1 Member, Instructor, Dept. of Civil Engrg., Chonnam National Univ., tkim@colorado.edu)
*2 Member, Associate Prof., Dept. of Civil Engrg., Seonam Univ.
*3 Member, Instructor, Dept. of Civil Engrg, Wonkwang Univ.

1. Introduction

It has been reported in numerous field observations and studies that the conventional analysis techniques used to evaluate the stability of slopes are inadequate for earth structures involving brittle soils such as cemented sands (Terzaghi, 1936; Skempton, 1964; Sitar et al., 1980), since this failure mode is characterized by fracture and not Mohr-Coulomb strength criterion implied in all slope stability analysis techniques. There might be several possibilities that lead to such an error or difference. Among them is the assessment of the factor of safety, which is assumed to be constant along the failure surface.

In limiting equilibrium analyses implemented in slope stability calculation, it is implicitly assumed that the stress-strain behavior of the soil is ductile, which means that there is still shear resistance after peak strength has been reached. If the shearing resistance drops off after reaching the peak, progressive failure can occur, and the shearing resistance that can be mobilized at some point may be smaller than the peak strength. In fact, many field observations showed that the average shear stress along the failure surface was much smaller than the shear strength estimated from laboratory tests. In conventional analysis, however, there is no standard approach to take into account this condition. The only approach is to use the residual strength rather than the peak strength in the analysis (Duncan, 1992). While modern finite element analysis techniques can account for the strain softening ductility is still assumed. The other possibility is that arbitrary assumptions of the failure surfaces of the slope are employed. The failures of steep slopes in cemented soils are, however, likely to be initiated by tensile splitting in the upper parts of the slope, and followed either by toppling or by shearing. Due to these possibilities, the prediction of slope stability has often failed and caused loss of a lot of life and property. In natural slopes of stiff soils, tension cracks are frequently observed. Early researchers have noticed that tension cracking behind the crests of slopes might be a possible factor that can lead to failure of slopes and vertical cuts, and therefore, that the fracture mechanics concept might be useful to examine possible cracking effect. However, most analyses were limited to simple cases such as opening mode with linear elastic behavior. A failure might, however, be dominated by more complicated mechanisms such as the combination of the opening mode (Mode I) and shear mode (Mode II). Therefore, a more comprehensive method such as nonlinear fracture mechanics with combined modes of fracture seems more appropriate. In this study, the stability of a nearly vertical cut slope as well as inclined slopes in cemented sand is analyzed using the so called interface crack model that has been modified from the original fictitious crack model to take into account the shear mode. The results are compared with the results calculated from conventional geotechnical slope stability analysis techniques. To do this, the general purpose finite element fracture analysis computer code, MERLIN and a commercial software, Geo-Slope, based on limiting equilibrium were used.

2. Geometry and Properties of Nearly Vertical Cut Slopes

Vertical cuts or almost vertical slopes in weakly cemented soils are common in the costal area of California (Sitar et al, 1980). Sitar and his colleagues observed that the slopes in this area are uncommonly high, and it is due to the fact that cementation increases strength and changes the failure mode. Through a series of laboratory tests and finite element analysis, they investigated the behavior of a vertical slope. According to the results of the finite element analysis, under at-rest gravity loads, a high tension zone is developed at the top of the crest, tension and shear zone at the slope surface about one third from the toe, and high shear zone at the toe. They considered these stresses relative to the shear strength of the soil. They argued that the shear stress at the toe would not lead to failure, because of the effect of confinement near the toe of the slope. They also concluded that a failure of a vertical slope in cemented soil could be initiated in the zone which is about one third from the toe. However since, as mentioned already earlier in this chapter, the field observations show that the

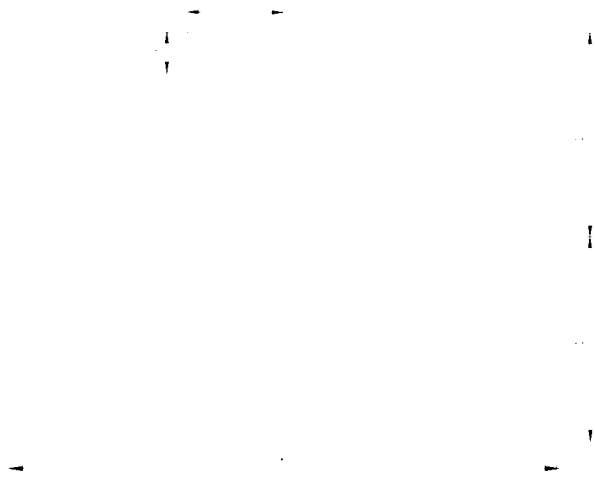

Fig. 1. Geometry and initial crack of a vertically cut slope

Table 1. Material properties

E (GPa)	γ_d (kN/m^3)	ν	c (kPa)	ϕ
3.17	19.7	0.3	143	35°

failures of steep slopes in cemented soils are apparently initiated by tensile splitting in the upper parts of the slope, this assertion may not be correct. In this study, the same vertical cut described by Sitar was used, and it is assumed that a crack is generated at the crest of the slope. The geometry of the vertical cut and an initial crack are shown in Fig. 1. The general material properties used in this application is shown in the Table 1.

3. Stability Assessment

3.1 Conventional Approach

In conventional slope stability analysis there are two major approaches. One is based on limit equilibrium and the other is based on limit plasticity, which considers the kinematical relationships. There are also several limit equilibrium methods. The most widely used approach is the methods of slices, which divide a slide-mass into several smaller slices. The greatest advantage of these methods is their ability to accommodate complex slope geometries, variable soil conditions, and the influence of external boundary loads. In contrast, there is also a shortcoming that the number of unknowns is larger than the number of equations. In general, there are (6n-2) unknowns, where n is the number of slides. However, there are only (4n) equations. Therefore the solution is statically indeterminate.

In order to solve this problem, the number of unknowns should be reduced, and this can be done by making some simplifying assumptions. Depending on the assumptions, the methods of slices are divided into several categories, such as Bishop's Method (Bishop, 1954), Ordinary Method of slices (Fellenius, 1927), Janbu's Method (Janbu, 1954), Spencer's Method (Spencer, 1967), etc. However, even though each of these methods is slightly different in some of the assumptions made, the methods are similar in the points that they involve a potential failure surface and that the shear strength required along the potential failure surface is calculated and then compared to the available shear strength.

Slope stability analyses are often assessed using published charts or for more complicated geometries and materials variations numerical analyses are used. In this section, the stability charts and approach generated by Janbu are introduced, because they are simple to use and, several different conditions such as surcharge loading at the top of the slope and tension cracks can be taken into account by the charts provided. In 1968, Janbu published stability charts for slopes in soils with uniform strength throughout the depth of the soil layer. A general notation for design is shown in Fig. 2, and the relative charts are provided in Fig. 3. Using these charts, the factor of safety of the vertical cut example could be obtained. The procedure is as follows.

- Fig. 3 provides the relationship between H_t/H and reduction factors (μ_1) due to presence of a tension crack. Therefore if the ratio is given, the reduction factor can be obtained from this chart.

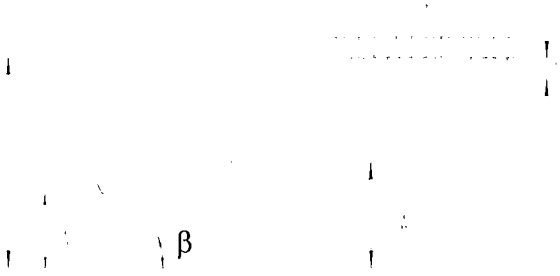

Fig. 2. Notations of slope for design

- Similarly, the relationship between $q/\gamma H$ and reduction factors (μ_q) is shown in Fig. 4. Again, using the given geometry, the reduction factor (μ_q) due to surcharge can be obtained.
- After obtaining the reduction factors, the design parameters P_d, P_e and $\lambda_{c\phi}$ are calculated from the chart shown in Fig. 5.

A stability number N_o is then obtained from the design shown in Fig. 5. Finally, the factor of safety is obtained using the equation given in Fig. 5.

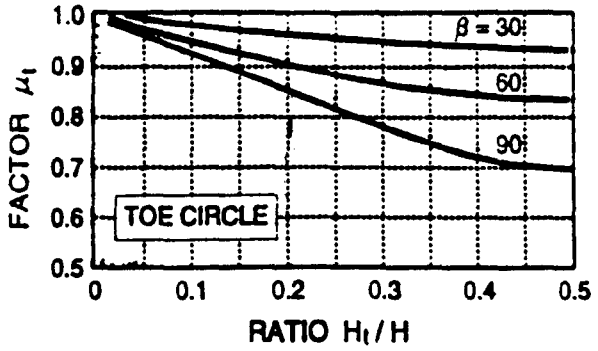

Fig. 3. Reduction factor for tension crack

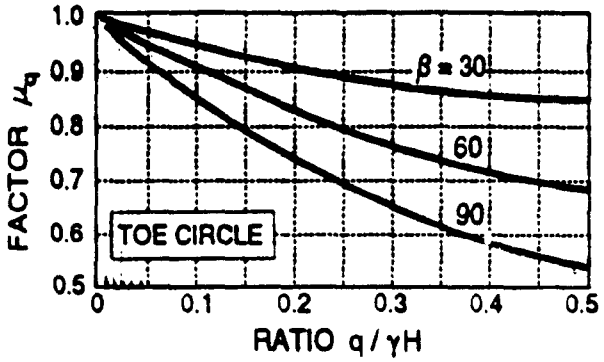

Fig. 4. Reduction factor for surchage

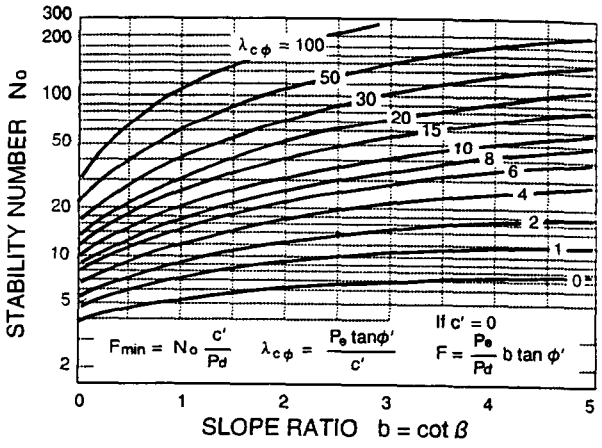

Fig. 5. Janbu's slope stability charts

3.2 Fracture Mechanics Approach

3.2.1 Nonlinear Finite Element Implementation

Fig. 6 shows a body consisting of two sub-domains. In general, the equation of equilibrium of a continuous system can be derived from the Principle of Virtual Work. The equation is

$$\int_{\Omega} \delta\varepsilon^T \sigma d\Omega - \int_{\Omega} \delta u^T b d\Omega - \int_{\Gamma_t} \delta u^T \hat{t}\, d\Gamma = 0 \tag{1}$$

Where,

Ω = the volume of the body

Γ_t = the surface of the body subject to prescribed surface traction

$\hat{t}$ = the prescribed surface traction

b = body force

In cracked body, however, additional integrals are required to account for the work performed by the surface tractions, which are normal and tangential stresses on the interface surface, and the work on the interface is written as

$$\int_{\Gamma_I} \delta u^T t_I d\Gamma = \int_{\Gamma_{Ib}} \delta u^T t_b d\Gamma + \int_{\Gamma_{IF}} \delta u^T t_F d\Gamma \tag{2}$$

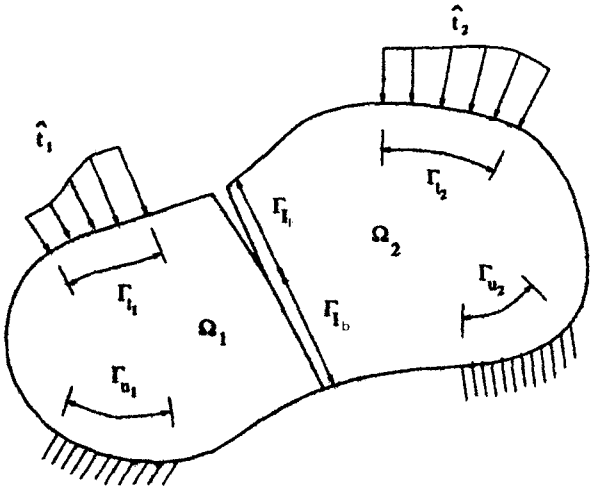

Fig. 6. Body consisting of sub-domains

Where,

Γ_I = the surface of the interface

Γ_{Ib} = the bonded interface surface

Γ_{IF} = the fracture process zone

t_I = the total surface traction on the interface

t_{Ib} = the traction on the bonded interface surface

t_{IF} = the traction on the fracture process zone

Both tIb and t_{IF} are unknown, but as t_{Ib} acts on the bonded interface it will be treated as a Lagrange multiplier. That is, $\lambda = t_{Ib}$.

Combining Eqs.(1) and (2), the equation of equilibrium of a cracked system can be rewritten as

$$\int_{\Omega}\delta\varepsilon^T\sigma d\Omega - \int_{\Omega}\delta u^T b d\Omega - \int_{\Gamma_t}\delta u^T \hat{t}\, d\Gamma - \int_{\Gamma_{Ib}}\delta u^T \lambda d\Gamma + \int_{\Gamma_{IF}}\delta u^T t_F d\Gamma = 0 \quad (3)$$

Eq. (3) can be rewritten in general form with indicial notation.

$$\int_{\Omega_i}\delta\varepsilon_i^T\sigma_i d\Omega - \int_{\Omega_i}\delta u_i^T b_i d\Omega - \int_{\Gamma_{ti}}\delta u_i^T \hat{t}_i\, d\Gamma - \int_{\Gamma_{Ibi}}\delta u_i^T \lambda_i d\Gamma + \int_{\Gamma_{IF_i}}\delta u_i^T t_{Fi} d\Gamma = 0 \quad (4)$$

By defining

$$u_i = N_{ui}\bar{u}_i,\ \delta u_i = N_{ui}\delta\bar{u}_i,\ \lambda = N_\lambda\bar{\lambda},\ \delta\lambda = N_\lambda\delta\bar{\lambda},\ \varepsilon_i = B\bar{u}_i,\ \sigma_i = E\varepsilon_i \quad (5)$$

The first term of Eq (4) can be rewritten as

$$\int_{\Omega_i}\delta\varepsilon_i^T\sigma_i d\Omega = \delta\bar{u}_i^T\int_{\Omega i}B_i^T E_i B_i d\Omega\bar{u}_i = \delta\bar{u}_i^T K_i\bar{u}_i \quad (6)$$

Where,

$$K_i = \int_{\Omega i}B_i^T E_i B_i d\Omega$$

Similarly,

$$\int_{\Omega_i}\delta u_i^T b_i d\Omega = \delta\bar{u}_i^T\int_{\Omega i}N_{ui}^T b_i d\Omega$$

$$\int_{\Gamma_{ti}}\delta u_i^T \hat{t}_i\, d\Gamma = \delta\bar{u}_i^T\int_{\Gamma ti}N_{ui}^T\hat{t}_i\, d\Gamma \quad (7)$$

Defining that

$$f_i = \int_{\Omega i}N_{ui}^T b_i d\Omega + \int_{\Gamma ti}N_{ui}^T\hat{t}_i\, d\Gamma \quad (8)$$

The second and the third terms in Eq. (4) is

$$\int_{\Omega_i}\delta u_i^T b_i d\Omega + \int_{\Gamma_{ti}}\delta u_i^T\hat{t}_i\, d\Gamma = \delta\bar{u}_i^T f_i \quad (9)$$

Again the external work due to surface traction on the interface is

$$\int_{\Gamma_{Ibi}}\delta u_i^T\lambda_i d\Gamma + \int_{\Gamma_{IF_i}}\delta u_i^T t_{Fi} d\Gamma = \delta\bar{u}_i^T(Q_i\bar{\lambda} + f_{Fi}) \quad (10)$$

Where, Q_i and f_{Fi} are the operator matrix for the load vectors due to surface tractions on the bonded interface and fracture process zone, and are defined as

$$Q_i = \int_{\Gamma_{Ibi}}N_{ui}^T N_\lambda d\Gamma,\ and \qquad f_{Fi} = \int_{\Gamma_{IF_i}}N_{ui}^T t_{Fi} d\Gamma$$

Finally, from Eqs. (6), (9), and (10), Eq. (4) can be rewritten as

$$\delta\bar{u}_i^T K_i\bar{u}_i - \delta\bar{u}_i^T f_i - \delta\bar{u}_i^T(Q_i\bar{\lambda} + f_{Fi}) = 0 \quad (11)$$

3.2.2 MERLIN FEM Code

In this study, the MERLIN FEM code developed at the University of Colorado at Boulder was selected. In

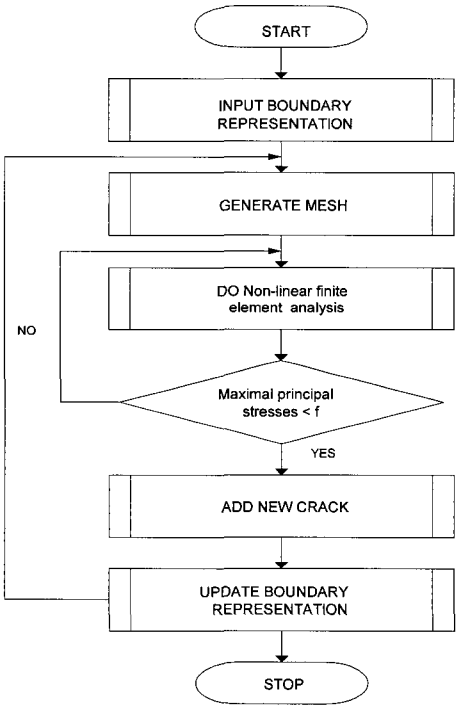

Fig. 7. Flow chart of the finite element analysis

the MERLIN code, a crack initiation and propagation is based on the stress based criterion. In other words, a crack is initiated when a maximal principal stress exceeds the tensile strength of the material. The procedure of finite element analysis is as follows. First a mesh is generated with initially given boundary representation, in which interface element are placed along the crack. Then, a nonlinear analysis is performed, and the maximal principal stresses at crack tips are monitored. This step is iterated until these stresses reach the tensile strength. Once the maximal principal stresses exceed the tensile strength, the analysis is interrupted. Then, a new crack of certain length is inserted into the boundary representation, and the same procedures are performed. This process is iterated until the structure is fully cracked or the prescribed loading level is reached. Fig. 7 shows the flow chart that described the process.

3.2.3 Stability Assessment

For the same example, FEM analysis based on nonlinear fracture mechanics concepts was performed. The initial mesh is shown in Fig. 8. In this analysis, the crack was first defined with ICM (Interface Crack Model). In ICM, a fracture process zone is modeled as a normal stress and a tangential stress that act to close a crack. These normal and tangential stresses are determined by softening laws that represent the relationship between the stresses to the relative displacements of the crack surfaces through the fracture energy. The material properties for this analysis,

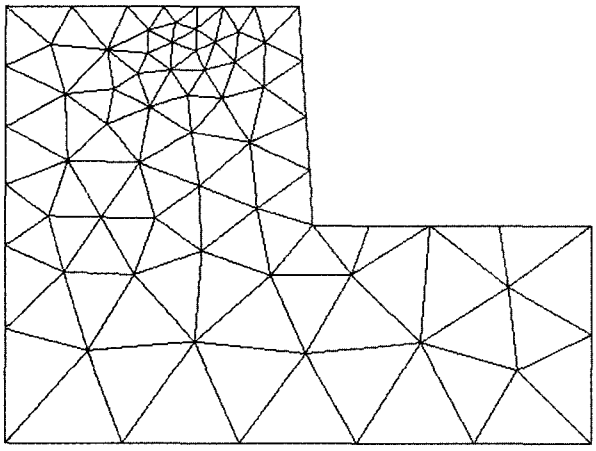

Fig. 8. Initial mesh of Slope

Table 2. Material properties used in fracture analysis

K_n (kPa/m)	K_t (kPa/m)	f_t (kPa)	G_I (N/m)	G_{II} (N/m)
3.17	3.17	20	0.013	0.13

normal stiffness (K_n), tangential stiffness (K_t), tensile strength (f_t), fracture energy (G), are shown in Table 2. After defining the crack, a nonlinear analysis was performed. In this study a stress based criterion was used. In other words, a crack is initiated when a maximal principal stress exceeds the tensile strength. Therefore during the analysis the maximal principal stress at the tip of the crack was checked for each load increment. Finally the safety factors were evaluated in terms of the ratio of the tensile strength to the tensile stress.

4. Discussion and Conclusion

The vertically cut slope described earlier with surcharge load applied at the crest was analyzed using conventional geotechnical strength-based limiting equilibrium techniques and a fracture mechanics approach. The surcharge was applied at the crest of the slope, and the magnitude of the surcharge was applied incrementally. Values of factors of safety were then evaluated using both approaches. The

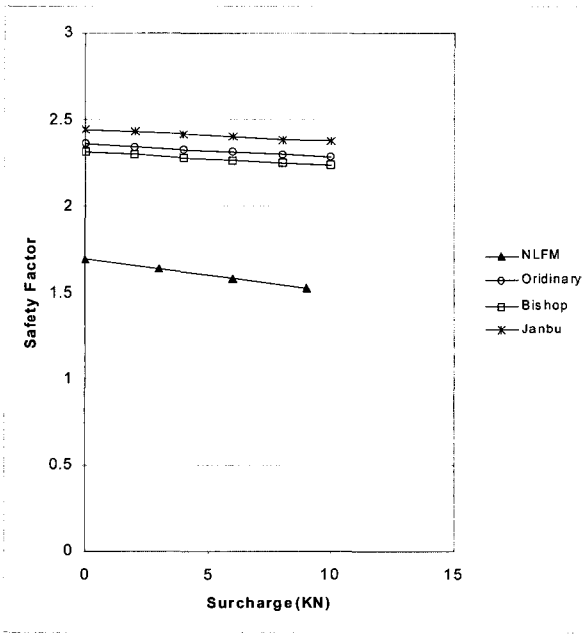

Fig. 9. Factor of safety vs. surcharge load

obtained values of factor of safety were plotted with respect to the surcharge in Fig. 9. It shows that the values of the factors of safety obtained from conventional geotechnical approaches are in the range 17% to 40% larger than those obtained from the fracture mechanics analysis. It also indicates that the safety factors obtained from fracture mechanics analysis decreases much faster than conventional geotechnical approaches as the surcharge increases. It might be because of localization of failure and stress concentration. The presence of cracks induces stress concentration. Such a phenomenon is increasing as load increases, and causes the faster crack propagation. In other words, the larger the surcharge load is, the higher the difference. In order to investigate the sensitivity of the safety factor to the surcharge load, the values of the factor of safety were normalized with respect to the safety factors, which were obtained under zero surcharge loads, and again plotted as shown in Fig. 10. This figure clearly indicates that fracture mechanics analysis is more sensitive to changes in loading than results obtained by conventional geotechnical stability analysis. In addition, in order to study if there was still significant difference in the factor of safety for more gentle slopes, a couple of cases, in which the slope angles were varied, were analyzed. Three different slope angles that include 60, 71 and 87 degree were selected. Fig. 11 shows normalized factors of safety with respect to surcharge for each case. This figure indicates that as the slope is becoming gentle, the sensitivity to change in loading is also becoming gentle and close to the results obtained by conventional geotechnical stability analysis. That might be because shear stress may much affect the failure in a gentle slope, while both tensile stress and shear stress affect the failure in a steep slope. However, it also shows that the fracture mechanics analysis is still sensitive to changes in loading. That is probably because, in fracture mechanics-based analysis, the strength reduction due to a discontinuity such as a crack is taken into account, which in turn results in a progressive failure state. On the other hand, in conventional geotechnical analyses, it is assumed that the shear strength of the soil is fully developed along the entire failure surface, and failure takes place simultaneously at all locations along the slope surface. Based on physical observations, it has been concluded that slopes usually fail by initiation and propagation of a crack rather than by the development of a slip surface. Thus, slope stability analysis with fracture mechanics appears to be more realistic as well as a useful tool in that it more accurately reflects what takes place.

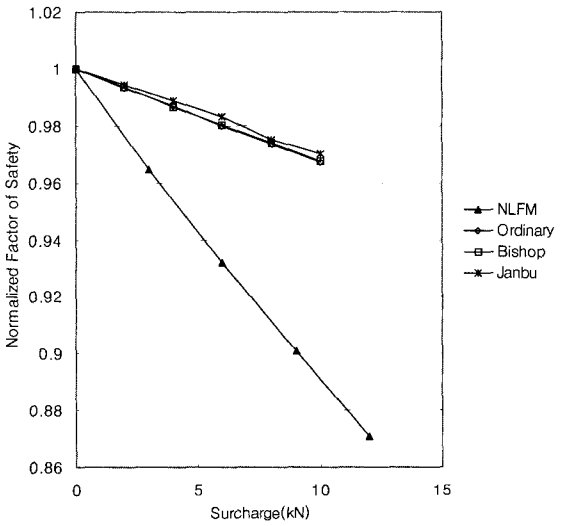

Fig. 10. Normalized factor of safety vs. surcharge load

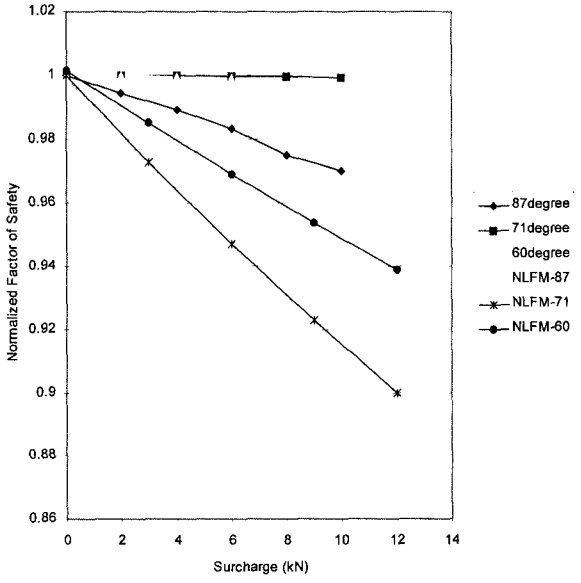

Fig. 11. Normalized factor of safety vs. surcharge load

References

1. Bishop, A.W.(1954), "The Use of the Slip Circle in the Stability Analysis of Slopes", *Geotechnique*, Vol.5.
2. Duncan, J.M.(1992), "State-of-the-Art: Static Stability and Deformation Analysis", ASCE, *Geotechnical Special Publication* No.31, "Stability and Performance of Slopes and Embankments-II", Vol.I, pp.222-266.
3. Fellenius, W.(1927), Erdstatische Berechnungen mit Reibung and Kohaesion, Ernst, Berlin.
4. Janbu, N.(1954), "Application of Composite Slip Surface for Stability Analysis", European Conference on Stability of Earth Slopes, Stockholm, Sweden.
5. Sitar, N., Clough, G.W., and Bachus, R.(1980), "Behavior of Weakly Cemented Soil Slopes Under Static and Seismic Loading Conditions", Final Report prepared for the United States Geological Survey, Dept. of Interior.
6. Skempton, A.W.(1964), "Long-term Stability of Clay Slopes", *Geotechnique*, Vol.14, pp.77-101.
7. Spencer, E.(1967), "A Method of Analysis of the Stability of Embankments Assuming Parallel Inter-Slice Forces", *Geothchnique*, Vol.17.
8. Terzaghi, K.(1936), "Stability of Slopes of Natural Clay", *Proc. of 1st Int. Conference of Soil Mechanics and Foundations*, Vol.1, paper No.G-7, pp.161-165.

(received on Jun. 15, 2003, accepted on Nov. 17, 2003)